VOL. 23, NO. 3, 2024, 84-91
elektrika.utm.my
ISSN 0128-4428

ELEKTRIKA
Journal of Electrical Engineering

Oscillation Control of a Double-Pendulum Overhead Crane Using Positive and Negative Input Shaping Techniques

Musa Mohammed Bello[1,2*], **Zaharuddin Mohamed**[1], **Haszuraidah Ishak**[1] and **Rania Mohammed Eltahir**[1]

[1]Faculty of Electrical Engineering, Universiti Teknologi Malaysia, 81310 UTM Skudai, Johor, Malaysia.
[2]Department of Mechatronics Engineering, Faculty of Engineering, Bayero University Kano, 3011, Kano, Nigeria.

[*]Corresponding author: bello.musa@graduate.utm.my

Abstract: A double-pendulum overhead crane system exhibits significant nonlinearity and is classified as an under-actuated system, making control more complex. This study focuses on designing a robust shaper to effectively mitigate oscillations in such systems. Two robust shapers, which are Zero Vibration Derivative (ZVD) and Negative Equal-Magnitude (NEM), are considered. These are obtained by convolving two input shapers that are designed based on the hook and payload oscillation frequencies. Matlab simulations are utilized to evaluate the performance of the shapers, using a nonlinear dynamic model of the crane to assess their effectiveness. Simulation results show that the ZVD shaper has a better performance in oscillation reduction, with 81% and 76% reductions for the hook and payload oscillations, respectively. In addition, the ZVD provides the lowest mean average error by achieving 87% and 83% reductions in the hook and payload as compared to the case with an unshaped input. However, the NEM shaper provides less delay in the trolley response.

Keywords: Double-pendulum, input shaping, negative equal-magnitude, overhead crane, robust shaper

Article History: received 9 July 2024; accepted 11 September 2024; published 30 December 2024

1. INTRODUCTION

Within the industrial sector, the application of flexible dynamic systems is widely applied. The control of said systems presents a significant challenge due to their inherently nonlinear and underactuated nature [1]. One of these systems is Crane. Cranes are commonly used in various industries such as warehouses, port facilities, construction sites, and nuclear power plants to transport heavy loads from one location to another. An Overhead crane is one type used in industries, particularly the manufacturing industry. The control of vibration and oscillation in these systems has been the subject of active research, and the control challenges increase for systems with two or more natural frequencies [2]. Double-pendulum cranes are examples of such systems. During motion, the double-pendulum crane operations involve coupled swings motion in the hook and payload. All the natural frequencies must be considered in the controller design for effective control of such systems. Researchers' control techniques for reducing load pendulation can be classified into closed-loop, open-loop and hybrid control techniques.

Different control techniques are employed in the close loop controllers. Some researchers have design feedback controllers based on the energy of the system to suppress the oscillation while assuming double pendulum swing dynamics [3] or controller that doesn't require retuning with the change in travel distance [4]. Adaptive controllers are also designed using sliding mode technique [5] to minimize the load swing in the presence of noise and large parametric uncertainties with fast and precise trolley positioning [6]. Precise trolley and with low load swing is achieved through robust non-linear controller [7]. Artificial intelligent techniques based on Fuzzy logic [8], Neural Network [9], are also implemented to eliminate the load pendulation. Researchers have also combined intelligent control techniques with classic controllers such as Genetic Algorithm with linear controller [10] and Fuzzy logic with non-linear controller [11] to stabilize the crane operation.

When compared to close loop techniques, open loop techniques are easier to implement [1]; however, simple input shaping techniques are not as robust, especially in the presence of parametric uncertainties and external noise. To take advantage of the ease of implementation of open loop control, researchers have developed new input shaping techniques that can withstand changes in certain parameters (like cable length and sway frequency) that might affect their performance. To eliminate load pendulation in cranes, Zero Vibration (ZV) and Zero Vibration Derivative (ZVD) input shapers are designed with distributed delay [12]. In order to achieve good positioning accuracy, input shaper impulses are modified online to account for the effect of weather conditions [13]. Uchiyama et al., [14] utilize an S-curve to reduce 2D residual load swing. The curve's parameters are derived through crane algebraic equation. Specified-

Negative-Amplitude (SNA) shaper was introduced in [15], it allows designers to fine-tune rise time, robustness, and high-mode excitation. The shaper was later tested on a robotic arm in [16], demonstrating faster rise times with reduced high-mode excitation, leading to improved performance. A research study by [17] investigated the use of input shapers, including both positive and negative types, to control vibrations in a flexible robot manipulator.

Some researchers have used combination of both open and close loop controller. In their work, [18] employed a closed loop controller to attain position accuracy and input shaping technique to eliminate motion induced oscillation. A hybrid control utilizing adaptive output-based command shaper with distributed delay was proposed in [19] to improved sway motion, and a PID controller was designed for trolley position control. Jafar et al., [20] combined a model reference command shaper with a feedback control scheme in other to achieved both precise position of trolley and low oscillation in hook and payload. Proposed in [21] is a linear matrix inequality based state feedback control that was designed to track the trolley position and to reduce the hook and payload oscillation.

This paper proposes the design of input shaping controllers to mitigate sway in overhead cranes. Two robust shapers are developed, Explicitly, Zero Vibration Derivative (ZVD) and Negative Equal-Magnitude (NEM) shapers, to achieve precise oscillation control. The comparison between the two input shapers is significant because it highlights their different characteristics, advantages, and limitations. This will help in making an informed decision, optimize system performance, and develop more effective control strategies in the future research. To design and examine the input shaping controllers for oscillation reduction, the system's response to a simple unshaped pulse input is initially analyzed to identify the system's key dynamic properties. Thereafter, the input shapers are tested in a simulation environment to measure their effectiveness in reducing swing angle and robustness. Finally, a comprehensive comparison of the control techniques is presented, evaluating their performance and reliability.

2. DOUBLE PENDULUM CRANE MODEL

The Lagrange method will be employed to develop a mathematical model of the double-pendulum overhead crane, as this approach has been extensively utilized and validated in previous studies [22]. The crane's configuration is characterized by three essential coordinates: x, representing the trolley's position, and the angular displacements θ and φ, describing the hook and payload, respectively. The crane system is characterized by seven essential parameters: the masses of the trolley, hook, and payload (m_t, m_h, m_p), the lengths of the two cable segments (l_1, l_2), the trolley's frictional force coefficient (f_x), and the gravitational constant (g). F_x, is the force applied to the crane, serving as the only control input for the system. Figure 1 shows a diagrammatic representation of a double-pendulum overhead crane system.

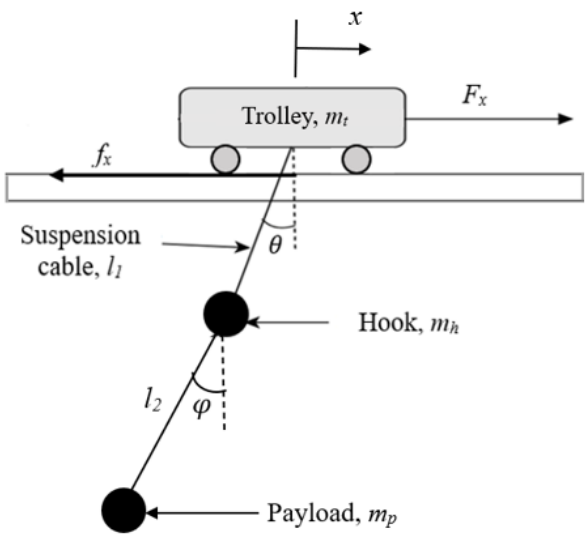

Figure 1. Double-pendulum overhead crane system

Lagrange's equation was used to obtain the equation of motion.

$$\frac{\mathrm{d}}{\mathrm{dt}}\left(\frac{\partial \mathrm{L}}{\partial \dot{\mathrm{q}}_\mathrm{i}}\right) - \frac{\partial \mathrm{L}}{\partial \mathrm{q}_\mathrm{i}} = \mathrm{T} \tag{1}$$

where L, q_i and T are the Lagrangian function, generalized coordinates and applied Torque respectively. The Lagrangian function can be stated as:

$$L = E_K - E_P \tag{2}$$

where E_K is the total kinetic energy and E_P is the total potential energy of the system. The system Kinetic energy can be obtained from Figure 1 as:

$$\begin{aligned} E_K = {} & \frac{1}{2}m_t\dot{x}^2 + \frac{1}{2}m_h\left[\dot{x}^2 + 2\dot{x}l_1\dot{\theta}cos\theta + l_1^2\dot{\theta}^2\right] + \\ & \frac{1}{2}m_p[\dot{x}^2 + 2\dot{x}l_1\dot{\theta}cos\theta + 2\dot{x}l_2\dot{\varphi}cos\varphi + l_1^2\dot{\theta}^2 + \\ & l_2^2\dot{\varphi}^2 + 2l_1l_2\dot{\theta}\dot{\varphi}cos(\theta - \varphi)] \end{aligned} \tag{3}$$

Similarly, from Figure 1 the potential energy can be obtained as:

$$\begin{aligned} E_P = {} & m_h[l_1(1 - cos\,\theta)] + m_p g[l_1(1 \\ & - cos\,\theta) + l_2(1 - cos\,\varphi)] \end{aligned} \tag{4}$$

Thus, the Lagrangian function can be written as:

$$\begin{aligned} L = {} & \frac{1}{2}m_t\dot{x}^2 + \frac{1}{2}m_h\left[\dot{x}^2 + 2\dot{x}l_1\dot{\theta}cos\theta + l_1^2\dot{\theta}^2\right] \\ & + \frac{1}{2}m_p[\dot{x}^2 + 2\dot{x}l_1\dot{\theta}cos\theta + 2\dot{x}l_2\dot{\varphi}cos\varphi + \\ & l_1^2\dot{\theta}^2 + l_2^2\dot{\varphi}^2 + 2l_1l_2\dot{\theta}\dot{\varphi}cos(\theta - \varphi)] - \\ & \{m_h[l_1(1 - cos\,\theta)] + m_p g[l_1(1 - cos\,\theta) \\ & + l_2(1 - cos\,\varphi)]\} \end{aligned} \tag{5}$$

Using equation (1) the mathematical model of the double-pendulum is obtained as follows:

$$(m_t + m_h + m_p)\ddot{x} + (m_h + m_p)l_1\ddot{\theta}cos\theta + m_p l_2\ddot{\varphi}cos\varphi - (m_h + m_p)l_1\dot{\theta}^2 sin\theta - m_p l_2\dot{\varphi}^2 sin\theta = F_x - f_x\dot{x} \quad (6)$$

$$(m_h + m_p)l_1\ddot{x}cos\theta + (m_h + m_p)\, l_1^2\, \ddot{\theta} + m_p l_1 l_2\ddot{\varphi}\, cos(\theta - \varphi) + m_p\, l_1 l_2\dot{\varphi}^2 \sin(\theta - \varphi) + (m_h + m_p)gl_1 sin\theta = 0 \quad (7)$$

$$m_p l_2\ddot{x}cos\varphi + m_p\, l_1 l_1^2\, \ddot{\theta}cos(\theta - \varphi) + m_p l_2^2\ddot{\varphi} - m_p\, l_1 l_2\dot{\varphi}^2 \sin(\theta - \varphi) + m_p g l_1 sin\varphi = 0 \quad (8)$$

Equations (6) – (8) presents the trolley position, hook oscillation and payload oscillation respectively.

Table 1. Parameters for double-pendulum overhead crane

Variables	Symbol	Values/Units
Mass of trolley	m_t	1.155 kg
Mass of hook	m_h	0.1 kg
Mass of payload	m_p	0.25 kg
Cable length between trolley and hook	l_1	0.3 m
Cable length between hook and payload	l_2	0.2 m
Viscous damping coefficients of trolley	fx	82 Ns/m
Gravitational constant	g	9.81 m/s^2

3. INPUT SHAPING TECHNIQUE

The basic concept behind input shaping technique is to try and control the system's input in order to reduce vibration. This technique has become popular among researchers due to its ability to move an underactuated system without causing vibration. The base command and the delay part of the base command are used to implement command shaping, which is an open-loop technique. This study investigates two types of robust input shaper, the goal is to identify the optimal impulse amplitudes and time locations. The objective is to mitigate the detrimental effects of system flexibility by determining parameters that account for the natural frequencies and damping ratios of the system.

3.1 Zero Vibration and its Derivatives

The formulations of the proposed technique for vibration and oscillatory control of flexible systems are presented in this section. Zero Vibration (ZV) is the simplest type of input shaping technique. For any system whose output can be expressed as:

$$y_0 = \frac{A_0\omega_n}{\sqrt{1-\zeta^2}} e^{-\zeta\omega_n(t-t_0)} \sin(\omega_n\sqrt{1-\zeta^2}(t-t_0)) \quad (9)$$

where A_0 is the amplitude of impulse applied, ζ the damping ratio and ω_n natural frequency of the system. Amplitude (A_i) and time location (t_i) of ZV shaped impulses are calculated by using the values of ζ and ω_n.

$$\begin{bmatrix} A_i \\ t_i \end{bmatrix} = \begin{bmatrix} A_1 & A_2 \\ 0 & t_2 \end{bmatrix} \quad (10)$$

where,

$$A_1 = \frac{1}{1+K}, \quad A_2 = \frac{K}{1+K}, \quad t_2 = \frac{\pi}{\omega_d} \quad (11)$$

with

$$\omega_d = \omega_n\sqrt{1-\zeta^2} \quad \& \quad K = e^{-\frac{\pi\zeta}{\sqrt{1-\zeta^2}}}$$

The amplitude and time location of ZV impulses is shown in Figure 2.

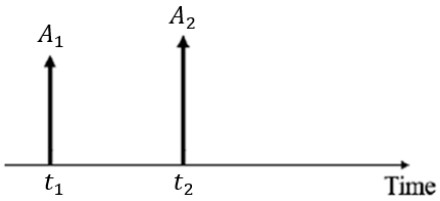

Figure 2. ZV Impulses

However, the ZV shaper is not robust because small adjustments/errors in damping ratio and natural frequency measurement degrade its performance. As a result, an additional constraint is proposed to improve the performance of the ZV shaper in the presence of nonlinearities, modelling errors, and parameter uncertainties [23]. This additional constraint causes the frequency derivative of residual vibration to become zero, thereby leading to an improved shaper known as Zero Vibration Derivative (ZVD) shaper technique. The ZVD implementation necessitates three impulses, the amplitude and time duration are determined from Equation (12),

$$\begin{bmatrix} A_i \\ t_i \end{bmatrix} = \begin{bmatrix} A_1 & A_2 & A_3 \\ 0 & t_2 & t_3 \end{bmatrix} \quad (12)$$

with

$$A_1 = \frac{1}{(1+K)^2}, A_2 = \frac{2K}{(1+K)^2}, A_3 = \frac{K^2}{(1+K)^2}, \quad t_2 = \frac{\pi}{\omega_d}, \quad t_3 = 2t_2$$

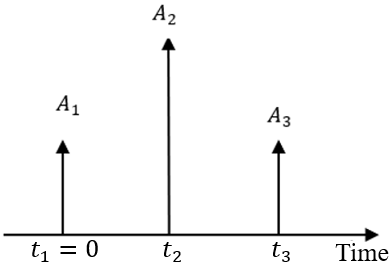

(a)

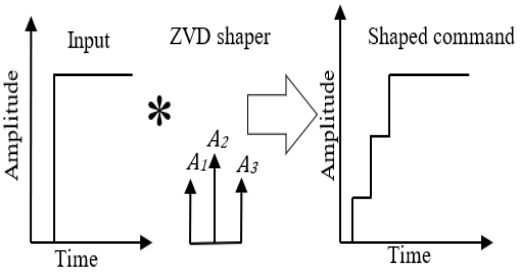

(b)

Figure 3. (a) ZVD shaper, (b) Shaping process

3.2 Negative Equal-Magnitude Shaper

The Negative Equal-Magnitude (NEM) shaper is a command shaping technique employed in motion control to mitigate vibrations and oscillations in mechanical systems, including crane operations, by shaping the command input to reduce unwanted motion. NEM shaper works by analysing the system's dynamics and natural frequencies, generating a command signal that cancels out the vibrations by applying an equal and opposite force which result to a smoother and more stable motion.

According to [24], the NEM shaper consists of three impulse vectors with specific magnitudes $I_1 = I\ (> 0)$, $I_2 = -I$, and $I_3 = I$ and with angles of $\theta_1 = 0$, $\theta_2 = {}^{\pi}/_{3}$, and $\theta_3 = {}^{2\pi}/_{3}$ respectively as shown in Figure 4.

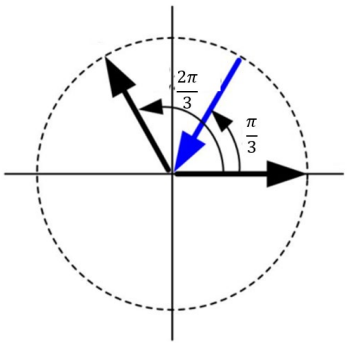

Figure 4. Impulse vector diagram for a NEM shaper with a negative impulse

The combined effect of the three impulse vectors cancels out, resulting in a net force of zero, which in turn eliminates any remaining vibrations. Based on these conditions, the NEM shaper can be derived, which consists of three impulse vectors as:

$$\begin{bmatrix} A_i \\ t_i \end{bmatrix} = \begin{bmatrix} I & \frac{-I}{\tau^{\frac{1}{3}}} & \frac{I}{\tau^{\frac{2}{3}}} \\ 0 & t_2 & t_3 \end{bmatrix} \tag{13}$$

where,

$$I = \frac{\tau}{(\tau + \tau^{\frac{2}{3}} + \tau^{\frac{1}{3}})}, \quad \tau = e^{\zeta\pi/\sqrt{1-\zeta^2}}, \quad t_2 = \frac{\pi/3}{\omega_d},$$
$$t_3 = \frac{2\pi/3}{\omega_d}$$

4. IMPLEMENTATION AND RESULTS

This section describes the research approach employed to develop and test the shapers, and reports the simulation results of the crane's oscillatory behavior. The controller's performance and robustness are analyzed and discussed in detail.

4.1 Research Tools

The study used the following research tools and techniques.

(a) The research utilized MATLAB/Simulink version R2021a software to simulate the nonlinear DPOC model Equations (6) – (8) and develop controller implementations.

(b) The ode45 solver, implementing the Dormand-Prince algorithm, was used to simulate the system with a variable time step size to ensure efficient and accurate results.

(c) A cable length between trolley and hook of 0.30 m and length between hook and payload of 0.20 m, with the hook mass (100 g), and payload mass (215 g), is use to investigate the dynamics of the system.

(d) The dynamic performance of the crane was evaluated by examining the time domain responses of the hook and payload, focusing on their oscillatory behaviour.

(e) Controller performance was evaluated based on two performance indices: Maximum Transient Sway (MTS) and Mean Absolute Error (MAE), which were calculated to assess controller effectiveness.

4.2 Implementation

This section presents the simulation outcomes generated using the MATLAB/Simulink environment. To simulate the movement of the trolley, a pulse input signal with a magnitude of 0.6 N and a duration of 2 s was applied to the crane as an external force, as shown in Figure 5. This simulated force represents a sudden and brief movement of the trolley, allowing for the analysis of the crane's dynamic response. The simulation results in Figure 6 (a) and (b) illustrate the oscillatory responses of the hook and

payload, respectively, in response to the input excitation shown in Figure 5.

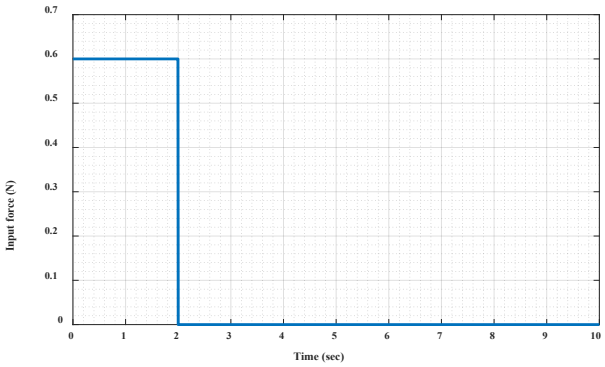

Figure 5. Input force signal

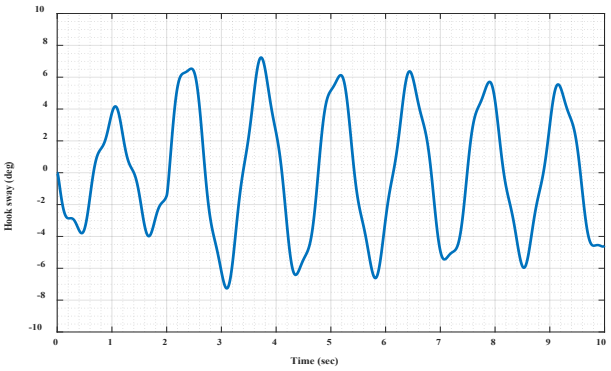

(a)

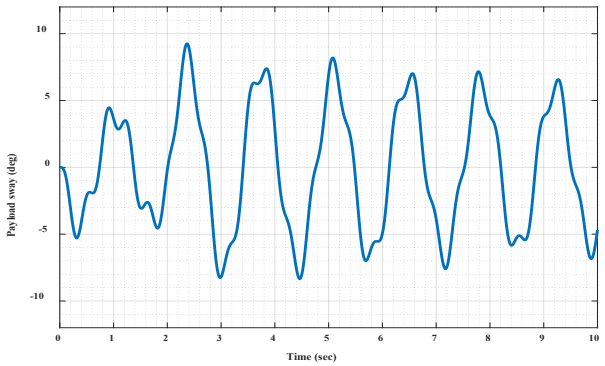

(b)

Figure 6. Unshaped response of the DPOC system (a) Hook oscillation and (b) Payload oscillation

Table 2. Hook and payload frequencies

Modes	ω_n (rad/s)	Zeta (ζ)
Hook	4.2481	0.0359
Payload	4.3348	0.0270

The simulation results in Figure 7 show the trolley's position responses to the input force, highlighting distinct transient behaviors but with identical steady-state responses. The unshaped input moves the trolley 0.29 m within 2 s, while the shaped inputs (NEM and ZVD) reach the same position, but with different settling times; NEM takes 2.5 s and ZVD takes 3 s. This suggests that the NEM shaper exhibits a more rapid response compared to the ZVD shaper. In general, negative shapers tend to have shorter shaping times compared to positive shapers, however, they are more sensitive to modelling errors and may excite high-frequency dynamics.

The natural frequency and damping ratio values presented in Table 2 will be substituted into Equations (12) and (13) to calculate the parameters needed to design the shapers. The calculated ZVD and NEM parameters presented in Table 3 are used to design separate shapers as described in section 3, the hook and payload shapers are merged using convolution, generating a multi-mode shaper, which then create a shaped input as shown in Figure 8, that is then used to simulate the trolley's movement.

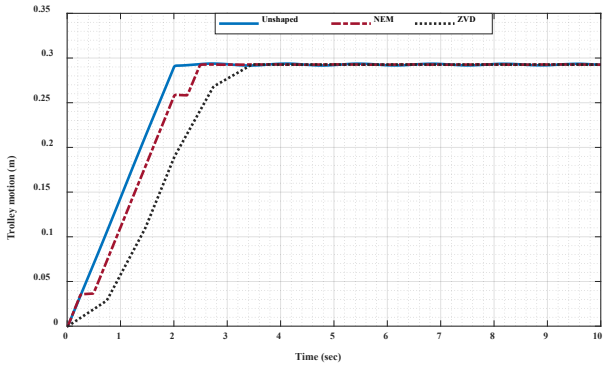

Figure 7. Trolley position response

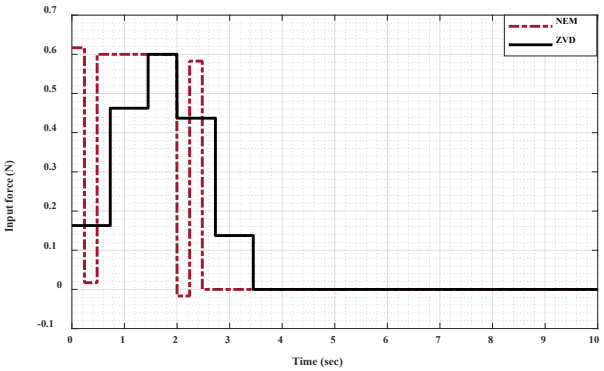

Figure 8. Shaped input force signal

Table 3. Shaper parameters for ZVD and NEM

Modes	Shapers	Magnitude			Time location	
		A_1	A_2	A_3	t_2	t_3
Hook	ZVD	0.27	0.5	0.23	0.73	1.45
	NEM	1.03	-0.99	0.97	0.24	0.48
Payload	ZVD	0.28	0.49	0.22	0.74	1.48
	NEM	1.04	-0.99	0.96	0.25	0.50

Figures 9 and 10 depict the simulations oscillation

response for the hook and payload, respectively. The results show that all the shapers consistently improve the system's performance when compared to the unshaped input, with ZVD demonstrating superior robustness and efficiency. The simulation results consistently indicates that ZVD outperforms NEM for both hook and payload responses, achieving a more substantial reduction in oscillation, making it a more dependable choice for system control.

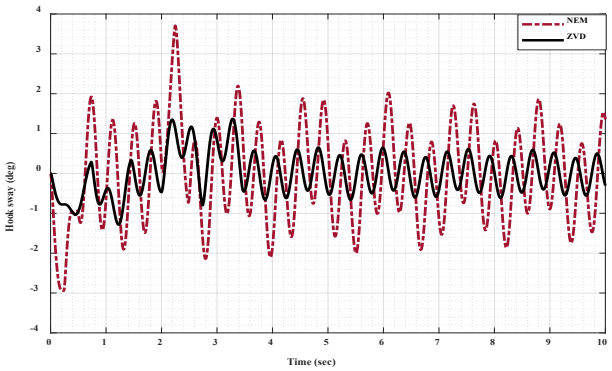

Figure 9. Hook oscillation response of DPOC system

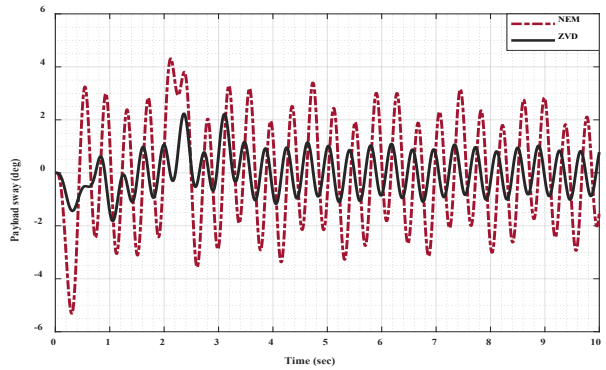

Figure 10. Payload oscillation response of DPOC system

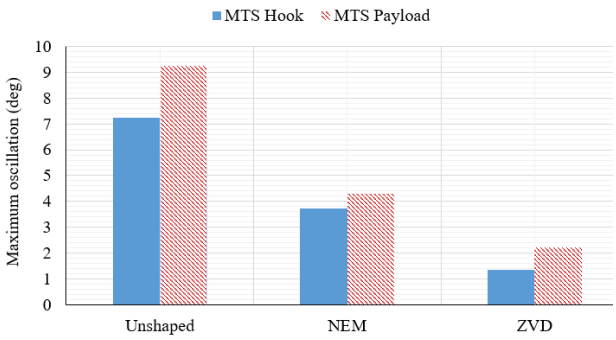

Figure 11. MTS of the crane oscillations with input shaper

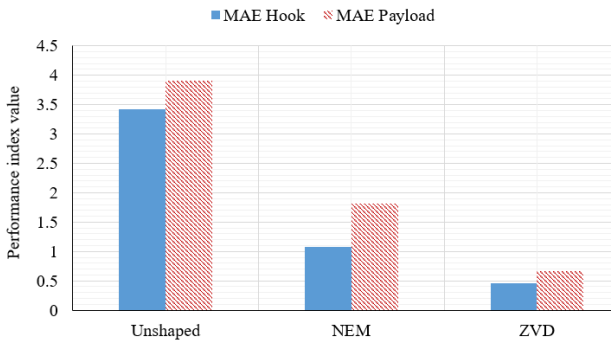

Figure 12. MAE of the crane oscillations with input shaper

Table 5 summarises overall MTS (MTS-O) and residual MTS (MTS-R) values. The total angle oscillations are examined over the initial 10 s period to obtained MTS-O values as presented in Figure 5, whereas for the MTS-R, the residual angle oscillations are assessed during the final second of the simulation, between 9 and 10 s. Table 6 gives the MAE values obtained using the shapers and their percentage of improvements as compared to the unshaped input. It can be shown that the ZVD provided the highest oscillation reduction with 83% reductions in the payload while NEM achieved 53% reduction.

Table 5. MTS-O and MTS-R values

Shapers	Hook (deg)		Payload (deg)	
	MTS-O	MTS-R	MTS-O	MTS-R
Unshaped	7.2364	5.49	9.2494	6.47
NEM	3.7187	1.53	4.3124	2.10
ZVD	1.3712	0.50	2.2320	0.83

Table 5. MAE Percentage improvement for hook and payload

Systems	Hook		Payload	
		%		%
Unshaped	3.4188	-	3.9050	-
NEM	1.0833	68.3	1.8209	53.4
ZVD	0.4612	86.5	0.6626	83

5. CONCLUSION

Zero Vibration Derivative (ZVD) and Negative Equal-Magnitude (NEM) input shapers have been successfully designed for robust oscillation control for an overhead crane system. MATLAB simulations using a nonlinear model of the crane showed that all shapers significantly reduced hook and payload oscillations compared to unshaped inputs. Furthermore, detailed analysis revealed that ZVD shapers outperformed NEM shaper, achieving the lowest values of MTS and MAE, demonstrating superior oscillation reduction capabilities.

REFERENCES

[1] L. Ramli, Z. Mohamed, A. M. Abdullahi, H. I. Jaafar, and I. M. Lazim, “Control strategies for crane systems: A comprehensive review,” *Mechanical*

Systems and Signal Processing, vol. 95, pp. 1–23, 2017.

[2] M. R. Mojallizadeh, B. Brogliato, and C. Prieur, "Modeling and control of overhead cranes: A tutorial overview and perspectives," *Annual Reviews in Control*, p. 100877, May 2023, doi: 10.1016/j.arcontrol.2023.03.002.

[3] N. Sun, Y. Fang, H. Chen, and B. Lu, "Amplitude-Saturated Nonlinear Output Feedback Anti-Swing Control for Underactuated Cranes with Double-Pendulum Cargo Dynamics," *IEEE Transactions on Industrial Electronics*, vol. 64, no. 3, pp. 2135–2146, 2017, doi: 10.1109/TIE.2016.2623258.

[4] X. Wu and X. He, "Nonlinear Energy-Based Regulation Control of Three-Dimensional Overhead Cranes," *IEEE Transactions on Automation Science and Engineering*, vol. 14, no. 2, pp. 1297–1308, 2017, doi: 10.1109/TASE.2016.2542105.

[5] A. T. Le and S. G. Lee, "3D cooperative control of tower cranes using robust adaptive techniques," *Journal of the Franklin Institute*, vol. 354, no. 18, pp. 8333–8357, 2017, doi: 10.1016/j.jfranklin.2017.10.026.

[6] N. Sun, Y. Fang, H. Chen, and B. He, "Adaptive nonlinear crane control with load hoisting/lowering and unknown parameters: Design and experiments," *IEEE/ASME Transactions on Mechatronics*, vol. 20, no. 5, pp. 2107–2119, 2015, doi: 10.1109/TMECH.2014.2364308.

[7] T. A. Le, V. H. Dang, D. H. Ko, T. N. An, and S. G. Lee, "Nonlinear controls of a rotating tower crane in conjunction with trolley motion," *Proceedings of the Institution of Mechanical Engineers. Part I: Journal of Systems and Control Engineering*, vol. 227, no. 5, pp. 451–460, 2013, doi: 10.1177/0959651812472437.

[8] H. M. Omar and A. H. Nayfeh, "Anti-swing control of gantry and tower cranes using fuzzy and time-delayed feedback with friction compensation," *Shock and Vibration*, vol. 12, no. 2, pp. 73–89, 2005, doi: 10.1155/2005/890127.

[9] S. C. Duong, E. Uezato, H. Kinjo, and T. Yamamoto, "A hybrid evolutionary algorithm for recurrent neural network control of a three-dimensional tower crane," *Automation in Construction*, vol. 23, pp. 55–63, 2012, doi: 10.1016/j.autcon.2011.12.005.

[10] M. I. Solihin, Wahyudi, M. A. S. Kamal, and A. Legowo, "Objective function selection of GA-based PID control optimization for automatic gantry crane," *Proceedings of the International Conference on Computer and Communication Engineering 2008, ICCCE08: Global Links for Human Development*, pp. 883–887, 2008, doi: 10.1109/ICCCE.2008.4580732.

[11] L. H. Lee, C. H. Huang, S. C. Ku, Z. H. Yang, and C. Y. Chang, "Efficient visual feedback method to control a three-dimensional overhead crane," *IEEE Transactions on Industrial Electronics*, vol. 61, no. 8, pp. 4073–4083, 2014, doi: 10.1109/TIE.2013.2286565.

[12] M. Maghsoudi, Z. Mohamed, M. Tokhi, A. Husain, and M. Abidin, "Control of a gantry crane using input-shaping schemes with distributed delay," *Transactions of the Institute of Measurement and Control*, vol. 39, no. 3, pp. 361–370, Mar. 2017, doi: 10.1177/0142331215607615.

[13] S. Garrido, M. Abderrahim, A. Gimenez, R. Diez, and C. Balaguer, "Anti-Swinging Input Shaping Control of an Automatic Construction Crane," *IEEE Transactions on Automation Science and Engineering*, vol. 5, no. 3, pp. 549–557, Jul. 2008, doi: 10.1109/TASE.2007.909631.

[14] N. Uchiyama, H. Ouyang, and S. Sano, "Simple rotary crane dynamics modeling and open-loop control for residual load sway suppression by only horizontal boom motion," *Mechatronics*, vol. 23, no. 8, pp. 1223–1236, 2013, doi: 10.1016/j.mechatronics.2013.09.001.

[15] W. Singhose and B. W. Mills, "Command Generation using Specified-Negative-Amplitude Input Shapers," in *Proceedings of the American Control Conference*, San Diego, California, Jun. 1999, pp. 61–65.

[16] W. Singhose, E. Biediger Ooten, Y.-H. Chen, and B. W. Mills, "Reference Command Shaping using Specified-Negative-Amplitude Input Shapers for Vibration Reduction," *Journal of Dynamic Systems, Measurement, and Control*, vol. 126, pp. 210–214, 2004.

[17] Z. Mohamed, A. K. Chee, A. W. I. M. Hashim, M. O. Tokhi, S. H. M. Amin, and R. Mamat, "Techniques for vibration control of a flexible robot manipulator," *Robotica*, vol. 24, pp. 499–511, 2006, doi: 10.1017/S0263574705002511.

[18] K. Sorensen, W. Singhose, and S. Dickerson, "A controller enabling precise positioning and sway reduction in bridge and gantry cranes," *Control Engineering Practice*, vol. 15, no. 7, pp. 825–837, 2007.

[19] A. M. Abdullahi, M. F. Hamza, Z. Mohammed, M. M. Bello, M. Attahir, and F. A. Darma, "Distributed delay adaptive output-based command shaping for different cable lengths of double-pendulum overhead cranes," *Int. J. Dynam. Control*, Aug. 2023, doi: 10.1007/s40435-023-01280-9.

[20] H. I. Jaafar, Z. Mohamed, M. A. Ahmad, N. A. Wahab, L. Ramli, and M. H. Shaheed, "Control of an underactuated double-pendulum overhead crane using improved model reference command shaping: Design, simulation and experiment," *Mechanical Systems and Signal Processing*, vol. 151, p. 107358, Apr. 2021, doi: 10.1016/j.ymssp.2020.107358.

[21] M. Muhammad, A. M. Abdullahi, A. A. Bature, S. Buyamin, and M. M. Bello, "LMI-Based Control of a Double Pendulum Crane," *Applications of Modelling and Simulation*, vol. 2, no. 2, pp. 41–50, 2018.

[22] H. I. Jaafar, Z. Mohamed, M. A. Shamsudin, N. A. Mohd Subha, L. Ramli, and A. M. Abdullahi, "Model reference command shaping for vibration control of multimode flexible systems with application to a double-pendulum overhead crane," *Mechanical Systems and Signal Processing*, vol. 115, pp. 677–695, Jan. 2019, doi: 10.1016/j.ymssp.2018.06.005.

[23] A. M. Abdullahi *et al.*, "Adaptive input shaping for sway control of 3D crane using a pole-zero cancellation method," in *2015 IEEE Student Conference on Research and Development*

(SCOReD), Kuala Lumpur: IEEE, Dec. 2015, pp. 134–138. doi: 10.1109/SCORED.2015.7449310.

[24] C.-G. Kang and S.-G. Lee, "Impulse Vector: A Basic Mathematical Tool to Design and Analyze Flexible Robots for Removing Residual Vibrations," in *2023 20th International Conference on Ubiquitous Robots (UR)*, Jun. 2023, pp. 6–12. doi: 10.1109/UR57808.2023.10202366.